IUE OBSERVATIONS OF OXYGEN-RICH SUPERNOVA REMNANTS

W.P. Blair[1], J.C. Raymond[2], J. Danziger[3], and F. Matteucci[3]

[1]The Johns Hopkins University
[2]Harvard-Smithsonian Center for Astrophysics
[3]European Southern Observatory

Oxygen-rich supernova remnants present an opportunity to observe material ejected in type II supernova explosions. IUE observations help to determine the composition of the ejecta (especially C and Si abundances) and to test models for the ionization and excitation of the ejecta. We present UV observations of two oxygen-rich supernova remnants (N132D in The Large Magellanic Cloud and 1E 0102-7219 in the Small Magellanic Cloud) and discuss the similarities and differences between them.

Keywords: nebulae:supernova remnants - nucleosynthesis - abundances

1. Introduction

A few supernova remnants (SNRs) contain remarkable high velocity knots of material entirely devoid of hydrogen and helium. At optical wavelengths these knots emit [O II] and [O III] lines most strongly, with weaker lines of neon, sulfer, calcium and argon in some cases (Refs. 6 and 13) and sometimes neutral oxygen recombination lines (Ref. 18).

The elemental composition of this high velocity material, undiluted since its ejection by the supernova explosion, provides a look at the products of nucleosynthesis inside the progenitor star before and during the explosion. It therefore provides a direct test of stellar evolution and nucleosynthesis calculations. Ultraviolet observations are extremely important for such tests, because all the strong emission lines of carbon, magnesium and silicon are located in the IUE wavelength range. In addition, ultraviolet observations can provide tests of models for the excitation and ionization of the ejcted material by shock waves (Refs. 6 and 11) or by photoionization (Ref. 3).

Of the seven remnants known to possess hydrogen-free knots, three are in our galaxy (Puppis A, Cas A and G292.0+1.8) and are unfortunately too highly reddened for IUE study. The SNR in NGC 4449 is extremely luminous intrinsically, but is so distant that only a weak detection of [O III] λ1663 was possible with IUE (Ref. 2). The Large Magellanic Cloud remnant 0540−69.3 is not only oxygen-rich, but also shows many similarities to the Crab Nebula; IUE observations of this object have been attempted twice, but only a faint continuum from the object has been detected (see Ref. 1). Only the supernova remnants N132D in The Large Magellanic Cloud and 1E 0102-7219 in The Small Magellanic Cloud are sufficiently bright and unreddened for detailed study with IUE. Below we discuss our IUE observations of these two objects and the conclusions that can be drawn from combined UV/optical data.

2. IUE Observations

Both N132D and 1E 0102-7219 show optical emission knots that are bright in the forbidden lines of oxygen and neon, with expansion velocities of 2250 and 6500 km s^{-1} and diameters of 32 and 6.9 pc, respectively (Refs. 7, 14 and 17). Although the exact relative line intensities differ, by-in-large the optical spectra are quite similar. This is in contrast to what we have found in the UV.

We have combined ESA and NASA shifts to obtain long SWP and LWP exposures on bright portions of O-rich material in each of these objects. The IUE spectra have been reduced from the extended line-by-line files at the RDAF at NASA/GSFC. Reseau marks, hits and hot camera pixels were removed from the line-by-line data before re-extracting the spectra. Figures 1a and 1b show the resulting SWP and LWP spectra of N132D, while Figure 2a and 2b show the corresponding spectra of 1E 0102-7219. Table 1 presents fluxes from these observations, which

correspond to the northeastern edge of the N132D ring and the southeastern side of 1E 0102-7219. The line intensities have not been corrected for reddening, but with E(B-V) = .08 − .09 (Refs. 3 and 14), the relative intensities of the UV lines are only marginally affected.

Comparison of the spectra and the line intensities shown in Table 1 indicates both similarities and differences in the emission from the two objects. Many of the same lines are seen although the relative intensities vary. No Si III] λ1982 emission is detected, so the λ1400 feature can be attributed to O IV] in both objects. Comparison of the observed line strengths indicates that the gas in 1E 0102-7219 has larger C, Ne and Mg abundances relative to O than in N132D by a factor of roughly two.

One of the most striking differences between the two spectra is the O I λ1356 line, which is at least twice as strong as O III] λ1663 in 1E 0102-7219, but entirely absent in N132D. This line is formed by recombination (Ref. 3), along with the optical λ7774 multiplet (Refs. 12 and 18). This identification is confirmed by optical spectra, which show the λ7774 line present in 1E 0102-7219 (Ref. 3), but not in N132D (unpublished spectrum). For the SMC remnant, the relative intensities of λ1356 and λ7774 can be used to scale the UV and optical line intensities, since these lines come from the same recombination cascade.

Another difference in the spectra is the presence of strong C II]λ2325 emission in N132D while none was detected in 1E 0102-7219. The presence of C II], C III] and C IV emission lines at comparable intensities in the UV spectrum of N132D (and the absence of the O I recombination lines) is a strong indicator that shock heating is responsible for exciting the emission in this object. The absence of C II] in the spectrum of the SMC remnant even though the carbon abundance is higher calls into question whether shocks are the main cause of the observed emission.

A related difference is apparent when the UV and optical line intensities are compared. In the SMC remnant, the UV lines are weaker than expected from most shock models with respect to the optical lines. The cleanest line ratio that demonstrates this is O III I(1663)/I(5007), which depends only on the temperature in the O^{2+} region. This ratio in 1E 0102-7219 is only 0.08 after reddening correction (Ref. 3). Shock wave models predict I(1663)/I(5007) in the range 0.3 − 0.9 (Refs. 6 and 12), which is difficult to avoid since the ratio is only weakly temperature dependent at electron temperatures high enough to collisionally ionize O^{+} to O^{2+}. For N132D we do not yet have an accurate UV to optical normalization, but from a crude comparison with the surface brightness estimate in Ref. 14, the ratio is between 0.15 and 0.60, roughly in accord with the expectations of shock heating.

3. Models and Interpretation

The differences mentioned above may well be related to differences in the mechanism exciting the emission in each object. The N132D observations were only made recently so we have not yet calculated detailed models for this object. Comparison of our observed UV line intensities to published models of a given shock velocity or set of assumed abundances (Refs. 6 and 12) do not provide a good match. However, the large IUE aperture no doubt samples material with a range of densities, shock velocities and compositions. The qualitative indicators discussed above provide convincing evidence that shock heating is the dominant excitation source in N132D.

Since 1E 0102-7219 is the strongest extended soft X-ray source in the SMC (Ref. 16), we consider fIX-ray photoionization models for this object. The 1.5×10^{37} ergs s^{-1} X-ray luminosity of 1E 0102.2-7219 (Ref. 9) implies an X-ray flux flux to density ratio far higher than in the other known oxygen-rich SNRs, and photoionization should be correspondingly more important. Detailed measurements of the X-ray spectrum are not available, so we have used the X-ray emission code described in Ref. 15 with updated atomic data summarized in Ref. 5 to generate model spectra covering the 5-1000 eV energy range at 2.1 eV resolution. Models of young SNRs generally show very strong emission from the helium-like ions of the elements present (e.g. Refs. 8 and 10) so we have added the emission of carbon in a 10^6 K plasma, oxygen at 1.6×10^6 K, and neon at 3×10^6 K to give a spectrum resembling those predicted by models. Several variants on this X-ray spectrum were used to examine the sensitivity of the results to the assumed X-ray spectrum. In particular, we tried much stronger carbon line emission, strong EUV emission in lines such as O V λ630, and attenuated EUV emission to simulate the effects of absorption by the optically bright gas. These alternatives changed the equilibrium temperatures of the photoionized gas by $\leq 30\%$ and some of the line ratios by factors of two, but they do not alter the general conclusions below.

The X-ray spectrum was used to compute the equilibrium ionization state and heating rate of gas at various densities, and the temperature was iterated until radiative cooling balanced the heating. The abundances assumed were appropriate for the ejecta from a Type II SN explosion. Some typical results of these models are as follows. The gas in the SMC remnant must span a wide range in density. Regions denser than about 10 cm^{-3} are needed to produce the O I recombination lines, but they are too cold to produce any line excitation except in the far infrared. Regions near 1 cm^{-3} are warm enough to produce the observed ultraviolet lines, but the temperatures are low enough that the UV to optical line ratios are modest. A fraction of order 10% of the apparent volume

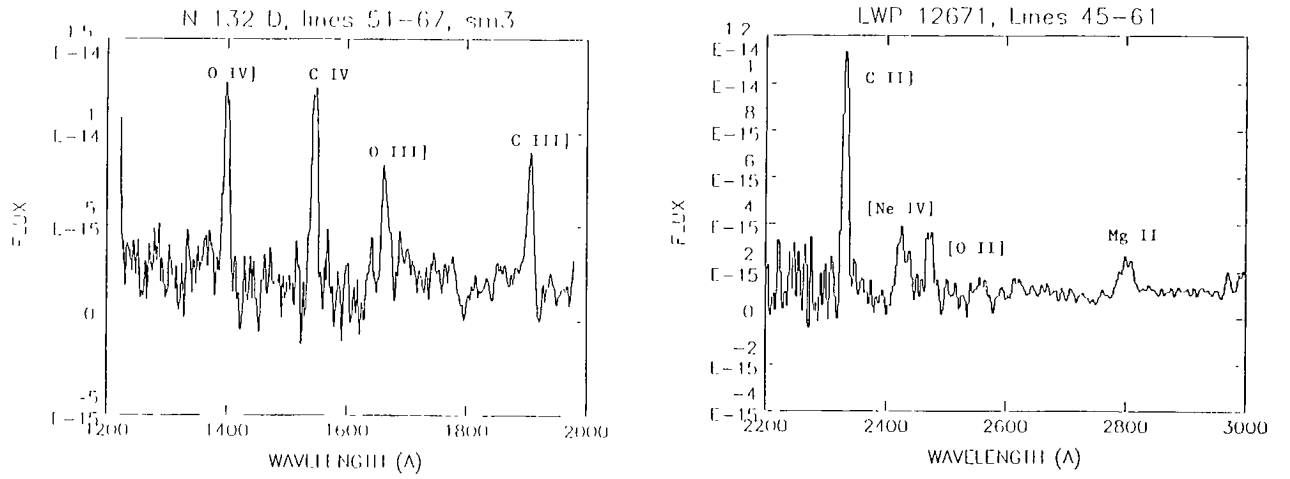

Figure 1: IUE spectra of N132D in the Large Magellanic Cloud. a) SWP 31578, 685 minute exposure. b) LWP 12671, 730 minute exposure. Hits and reseau marks have been removed and the data have been smoothed over three pixels.

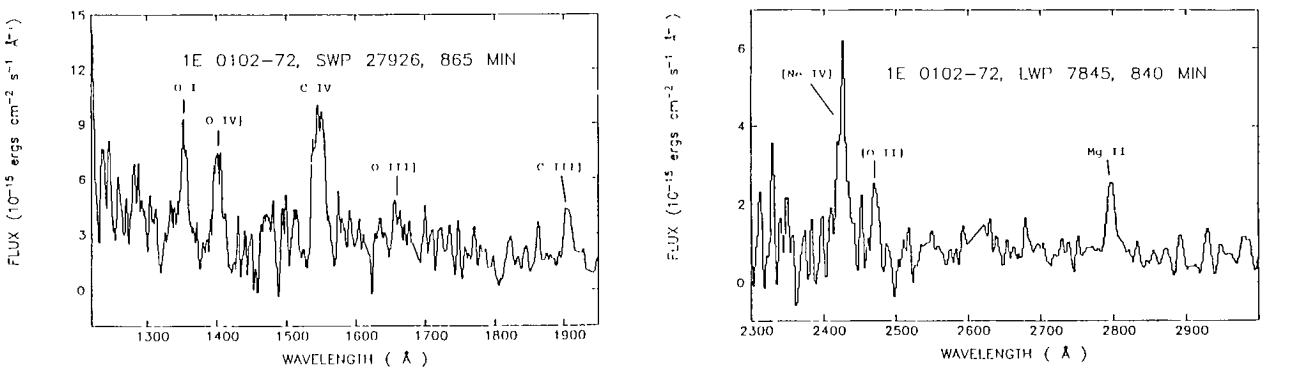

Figure 2: IUE spectra of 1E 0102-7219 in the Small Magellanic Cloud. a) SWP 27926, 865 minute exposure. b) LWP 7845, 840 minute exposure. Hits and reseau marks have been removed and the data have been smoothed over three pixels.

Table 1

Ultraviolet Emission Line Intensities for O-rich SNRs

Relative to O III] λ1663 = 100

Ion	Wavelength	1E 0102 − 7219	N132D
C II	λ1335	<40	<8
O I	λ1356	204	<13
O IV], Si IV	λ1400	328	152
C IV	λ1550	600	179
He II	λ1640	<27	<13
O III]	λ1663	100	100
N III]	λ1750	<27	<13
Si III]	λ1892	<13	<10
C III]	λ1909	133	101
C II	λ2325	<67	152:
[Ne IV]	λ2425	191	73
[O II]	λ2470	62	58
Mg II	λ2800	74	44
F(O III] λ1663) (in ergs cm^{-2} s^{-1})		2.6 E −14	7.7 E −14

of a torus 3.5 pc in radius with a minor radius one tenth as large containing gas at a density $n_o \sim 1$ cm^{-3} can account for the observed [O III] optical luminosity, and similar volumes at higher densities can produce the oxygen recombination radiation and the UV lines.

There are two major difficulties with the equilibrium photoionization models. First, the [O II]λ3727/[O III]λ5007 ratio is predicted to be less than about 0.3, while the observed ratio varies between 1.3 and 2. This reflects the fact that oxygen is mostly doubly ionized in models warm enough to effectively excite the λ3727 transition. Second, the [O III] emission comes mostly from 10,000 - 15,000 K gas in the model, but the I(4363)/I(5007) ratio suggests a temperature of 25,000 K.

Both difficulties may be related to an unwarranted assumption of ionization equilibrium. While the heating and cooling timescales are a few years, so that thermal balance is a valid approximation, the ionization timescales are ∼ 2000 years, which is close

to the expansion age of 1E 0102-7219. Hence, time dependent models should give a lower ionization state than predicted by the equilibrium model and also be somewhat warmer. We have run a series of time-dependent photoionization models where gas having the same abundances as above was allowed to expand freely at 3900 km s^{-1} for 2400 years while exposed to the X-ray flux described above. The gas was initially taken to be cold and neutral, but the initial conditions turned out to be irrelevant since the gas always cooled quickly, then slowly warmed and ionized late in the evolution.

Again, these models indicate that a mixture of densities is needed to produce both the high ionization lines and the O I recombination lines. These particular models improve the [O II]/[O III] ratio, but still fall short of the observed value. They also predict a larger C III]/C IV ratio than observed and far too much C II] λ2325. These problems could be alleviated by increasing the carbon line intensities and decreasing the oxygen lines in the ionizing X-ray spectrum. However, considering the large number of free parameters, we are loath to adjust the model parameters to try to "fit" the observed spectrum.

In summary, time-dependent photoionization by the EUV and X-ray radiation from 1E 0102-7219 can qualitatively explain its UV and optical line emission, but the density and ionization structures are complex and prevent a unique model from being specified. Many model parameters are poorly constrained, including the time dependence and shape of the ionizing spectrum. Moreover, the models presented here are not self-consistent in that the volumes and densities of the optically emitting gas imply optical depths of order unity in the EUV, but absorption of the ionizing radiation has been ignored.

It is possible that these shortcomings reflect a more fundamental limitation of the model assumptions. We have assumed throughout that the electron velocity distribution is Maxwellian and that the energy deposited by photoionization heats the electrons directly. In fact, the ~ 500 eV electrons produced by the Auger process may excite or ionize other ions before they slow down enough to share their energy with other electrons. Many of the excitations would produce photons that could ionize lower ionization stages.

Our inability to define a unique model for either of these objects at present may also be related to the complexity of the objects themselves. It may be that shocks and photoionization are needed to explain the emission from the SMC remnant. Spatial variations in composition or physical conditions such as are seen in Cas A (Ref. 4) would tend to be averaged together in our IUE large aperture spectra, which incorporate a fair fraction of the emission from each object; this would make a unique interpretation very difficult. Also, differences in aperture positions and sizes between UV and optical spectra can cause confusion if spatial variations are present. Higher spatial resolution observations and combined UV/optical coverage with the same aperture sizes will be strengths of the Faint Object Spectrograph on the Hubble Space Telescope, and we plan to continue these studies with that instrument when it becomes available.

It is a pleasure to thank the dedicated staff of the IUE Observatory on both sides of the Atlantic for their part in helping procure the ultraviolet data. This project has been supported by the following grants: NAG 5-701 and NAG 5-988 to The Johns Hopkins University, and NAG 5-87 to the Smithsonian Astrophysical Observatory.

4. References

1. Blair W P & Panagia N 1987, in *Exploring the Universe with the IUE Satellite*, Y Kondo (Ed), Dordrecht, D. Reidel Publ. Co., 549.
2. Blair W P et al 1984, *Ap J.* **279**, 708.
3. Blair W P et al 1988, *Ap J.* Submitted.
4. Chevalier R A & Kirshner R P 1978, *Ap J.* **219**, 931.
5. Cox D P & Raymond J C 1985, *Ap J.* **298**, 651.
6. Dopita M A et al 1984, *Ap J.* **282**, 142.
7. Dopita M A & Tuohy I R 1984, *Ap J.* **282**, 135.
8. Hamilton A J S et al 1983, *Ap J Suppl.* **51**, 115.
9. Hughes J P 1987, *Ap J.* **314**, 103.
10. Hughes J P & Helfand D J 1985, *Ap J*, **291**, 544.
11. Itoh H 1981, *Pub A S J.* **33**, 1.
12. Itoh H 1986, *Pub A S J.* **38**, 717.
13. Kirshner R P & Chevalier R A 1977, *Ap J.* **218**, 142.
14. Lasker B 1980, *Ap J.* **237**, 765.
15. Raymond J C & Smith B W 1977, *Ap J Suppl.* **35**, 419.
16. Seward F D & Mitchell M 1981, *Ap J.* **243**, 736.
17. Tuohy I R & Dopita M A 1983, *Ap J Letters.* **268**, L11.
18. Winkler P F & Kirshner R P 1985, *Ap J.* **299**, 981.